Доклади на Българската академия на науките
Comptes rendus de l'Académie bulgare des Sciences

Tome 66, No 3, 2013

SCIENCES ET INGENIERIE

Mécanique

ANALYTICAL PULLOUT ANALYSIS FOR CARBON NANOTUBE-CEMENT COMPOSITES UNDER STATIC LOADING

Zenon Mróz, Ana Yanakieva*, Varbinka Valeva*, Jordanka Ivanova*

(*Submitted by Corresponding Member A. Baltov on November 28, 2012*)

Abstract

The paper presents analytical pullout analysis for Carbon nanotube-cement composite based on Shear-lag assumptions. The composites under study are cement matrix composites reinforced by means of unidirectional Carbon nanotubes (CNT). The interface is assumed to be a material line with constitutive behaviour characterized by a relation between sliding stress and relative sliding displacement. Frictional sliding at the interface region is described by three different interface models: (i) Constant-τ model; (ii) Linear slip-hardening model and, (iii) Linear slip-softening model. The pullout analysis is performed considering static loading. The numerical examples are performed for concrete geometrical and material characteristics for CNT/cement composite. The obtained results are illustrated by figures and discussed.

Key words: Shear-lag model, interface sliding models, static loading, pullout analysis, Carbon nanotube cement reinforced composites

1. Introduction. In general, Carbon nanotubes (CNTs) as reinforcing material are used in four types of matrices – polymer, metal, ceramic and cement. The most widely studied ones are polymer composites, second of interest are both metal and ceramic composites and the rarest data are those on cement composites. A new area of research for experimental, theoretical and numerical investigations involves CNT/cement systems. The ordinary Portland cement is extensively used

This work was supported by KMM-VIN through a KMM-VIN Research Fellowship 2011.

worldwide for building and construction. However, it has limited structural applications because of poor tensile strength and strain capacity [1]. Recent research has shown that the incorporation of CNTs in cement is a novel way to improve material mechanical and durability properties. CNT are expected to have several distinct advantages as a reinforcing material for cements as compared to more traditional fibres: (1) they possess strength significantly greater than that of other fibres [2]; (2) their much higher aspect ratios require significantly higher energy of crack propagation [3]; (3) owing to their smaller diameters, they can reduce porosity of the matrix, and CNT diameters, being close in size to the thickness of the calcium silicate hydrate layers, may show very different bonding mechanisms and reduce the volume of the structural material; (4) they improve the transport properties of the composite by increasing the early age strain capacity of the cement matrix [4].

The good understanding of pullout behaviour plays an important role in the further investigation of the entire RC system, regarding its strength and fracture toughness.

A number of analytical and numerical models can be found in literature where the pullout behaviour is investigated. In [5] the pullout model considering nonlinear in-plane stiffness in the axial direction and effective stiffness in the circumferential direction for multi-walled CNTs is created. Papers [6–8] present analytical models where the mechanical properties of composite are considered by taking into account the morphology of the CNT. The effect of NT curvature on nanocomposite toughness is studied on the basis of classic Shear-lag assumptions. Computer simulation of carbon nanotube pullout from polymer by means of the molecular dynamics method can be found in [9]. The interfacial shear strength has also been estimated via the change of total potential energy. The pullout model for inclined carbon nanotube/fibre is developed in [10–12]. The pullout model predicts higher pullout forces as the fibre curvature increases and a lower pullout force in the case of a fibre with zero curvature. The analysis is based upon Lawrence model [13] and Shear-lag assumptions. Inertial effects in the mechanism of fibre pullout during the dynamic propagation of a bridged crack are examined by employing simple Shear-lag models of pullout during dynamic wave propagation. Using the methods of complex function, the bridging pullout of a composite material is transformed into the dynamic model involving the Reimann–Hilbert mixed boundary value problem. In the most cases, analytical and numerical analyzes [14] consider the frictional sliding at the interface region as being uniform or the so-called "Constant-τ model", assuming that $\tau = \tau^{\mathrm{cr}}$ for all values of sliding displacement (S) during the pullout process. Unfortunately, experimental knowledge on CNT composites related to CNT pullout behaviour is very restricted, especially for CNT/cement systems [15–18].

The aim of the present research is to propose analytical pullout analysis of CNT/cement composites based on Shear-lag assumptions for three different

interface models: (i) Constant-τ model; (ii) Linear slip-hardening model and, (iii) Linear slip-softening model. The composites under study have a cement matrix and are reinforced by means of unidirectional CNTs. The interface is assumed to be a region with constitutive behaviour characterized by a relation between sliding stress (τ) and sliding displacement (S). The pullout analysis is performed considering a static loading case.

2. Analytical models. A representative unit composite cell is shown in Fig. 1. It is assumed that both CNT (further, it will be used the term "fibre") and the matrix have an elastic behaviour with moduli E_f and E_m, respectively. Two main stages develop in the interface region during the entire loading process – slip stage (with partial bonded and debonded parts) and pullout stage. The model does not take into account the effect of Poisson's ratio of the matrix and the fibre is frictionally bonded to the matrix.

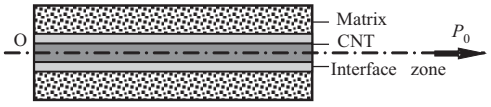

Fig. 1. Representative composite unit cell

The relation between interfacial sliding stress (τ) and interfacial sliding displacement (S) gives information about the fibre/matrix interface, where (S) is the relation between fibre axial displacement and the matrix $S = u_f - u_m$.

The following parameters are also introduced: $\alpha = 2/r_f$, $\beta = 2r_f/(r_m^2 - r_f^2)$, $\eta = A_f E_f / A_m E_m$, $\omega = \sqrt{k_c \left(\dfrac{\alpha}{E_f} + \dfrac{\beta}{E_m} \right)}$, where r_f and r_m are the radii of the fibre and the matrix, $A_f = \pi r_f^2$, $A_m = \pi(r_m^2 - r_f^2)$.

The equilibrium Shear-lag equations and constitutive laws for axial stresses of CNT and matrix are

$$\frac{d\sigma_f}{dx} - \alpha\tau = 0 \quad \text{and} \quad \frac{d\sigma_m}{dx} + \beta\tau = 0; \tag{1}$$

$$\sigma_f = E_f \frac{\partial u_f}{\partial x} = E_f \varepsilon_f \quad \text{and} \quad \sigma_m = E_m \frac{\partial u_m}{\partial x} = E_m \varepsilon_m. \tag{2}$$

Three constitutive models are assumed to describe the interface behaviour.

2.1. Case 1 – Constant model.

$$\tau = \tau^{\mathrm{cr}} = \text{const} \tag{3}$$

Slip stage.

The boundary conditions for that stage are $\sigma_f|_{x=l} = P/A_f = \sigma_0$ and $\sigma_m|_{x=l} = 0$. So, the solutions for axial stress in the fibre and matrix for the whole slip stage are

$$\sigma_f = -\alpha\tau^{\mathrm{cr}}(l - x) + \frac{P}{A_f} = \sigma_0 - \alpha\tau^{\mathrm{cr}}(l - x); \tag{4}$$

$$\sigma_m = \beta\tau^{\mathrm{cr}}(l - x). \tag{5}$$

We assume $u_f = u_m$ or $\varepsilon_f = \varepsilon_m$ to be the displacements in that zone, and thus

$$\frac{\sigma_f}{E_f} = \frac{\sigma_m}{E_m}. \tag{6}$$

Then, the following expression can be derived from equations (4) and (5)

$$\sigma_0|_{x=0} = \tau^{\mathrm{cr}} l \left(\alpha + \beta\frac{E_f}{E_m}\right). \tag{7}$$

So, we find the following form of the pullout force

$$P = \sigma_0 A_f = \tau^{\mathrm{cr}} l \left(\alpha + \beta\frac{E_f}{E_m}\right) A_f. \tag{8}$$

To derive the displacements in the fibre and in the matrix, equations (4) and (5) are used. The substitution of (4) and (5) into (6) yields

$$S = \frac{\tau^{\mathrm{cr}} x^2}{2E_f}\left(\alpha + \beta\frac{E_f}{E_m}\right) \tag{9}$$

and

$$\sigma_0 = \sqrt{2E_f\tau^{\mathrm{cr}}\left(\alpha + \beta\frac{E_f}{E_m}\right)S} = \tau^{\mathrm{cr}} x\left(\alpha + \beta\frac{E_f}{E_m}\right). \tag{10}$$

Pullout stage (see Fig. 2).

(11)

$$\sigma_0 = \alpha(1+\eta)\int_{\delta - S_{\mathrm{om}}}^{l} \tau(x)\,dx = \alpha(1+\eta)\tau^{\mathrm{cr}} x\Big|_{\delta - S_{\mathrm{om}}}^{l} = \alpha(1+\eta)\tau^{\mathrm{cr}}[l - (\delta - S_{\mathrm{om}})];$$

$$S\big|_{x=l} = S_{\mathrm{om}} = \frac{\tau^{\mathrm{cr}} l^2}{2E_f}\left(\alpha + \beta\frac{E_f}{E_m}\right); \tag{12}$$

$$\sigma_0 = \alpha(1+\eta)\tau^{\mathrm{cr}}[l - (\delta - S_{\mathrm{om}})]. \tag{13}$$

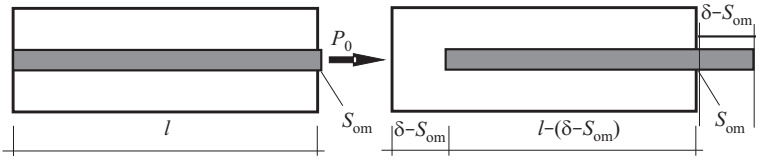

Fig. 2. *a*) Initial pullout state; *b*) Pullout stage

2.2. Case 2 – Linear slip-hardening model.

$$\tau = \tau^{\mathrm{cr}} + k_c S, \quad \tau = \tau^{\mathrm{cr}} + k_c(u_f - u_m). \tag{14}$$

Putting (2) into (1) we get

$$E_f(u_f)'' - \alpha\tau = 0 \quad \text{and} \quad E_m(u_m)'' + \beta\tau = 0. \tag{15}$$

After performing a transformation of equation (15) and employing equation (14) we obtain the following nonhomogeneous equation:

$$S'' - k\left(\frac{\alpha}{E_f} + \frac{\beta}{E_m}\right) S = \tau_c \left(\frac{\alpha}{E_f} + \frac{\beta}{E_m}\right). \tag{16}$$

Slip stage. The solution of equation (16) for slip stage, considering the same boundary conditions as those used in the previous interface model, takes the form

$$S = \frac{\tau^{\mathrm{cr}}}{k_c}[\cosh(\omega x) - 1], \tag{17}$$

$$\sigma = \frac{\tau^{\mathrm{cr}}\alpha}{\omega}(1+\eta)\sqrt{2\frac{k_c S}{\tau^{\mathrm{cr}}} + \left(\frac{k_c S}{\tau^{\mathrm{cr}}}\right)^2}. \tag{18}$$

Pullout stage.

$$S_{\mathrm{om}} = \frac{\tau^{\mathrm{cr}}}{k_c}[\cosh(\omega l) - 1], \quad S = \frac{\tau^{\mathrm{cr}}}{k_c}[\cosh(\omega x) - 1] + \delta - S_{\mathrm{om}}; \tag{19}$$

$$\sigma_{\mathrm{om}} = \frac{\tau^{\mathrm{cr}}\alpha}{\omega}(1+\eta)\sqrt{2\frac{k_c S_{\mathrm{om}}}{\tau^{\mathrm{cr}}} + \left(\frac{k_c S_{om}}{\tau^{\mathrm{cr}}}\right)^2}; \tag{20}$$

$$\tau = \tau^{\mathrm{cr}} + \tau^{\mathrm{cr}}[\cosh(\omega x) - 1] + k_c(\delta - S_{\mathrm{om}}) = \tau^{\mathrm{cr}}\cosh(\omega x) + k_c(\delta - S_{\mathrm{om}}); \tag{21}$$

$$\begin{aligned} \sigma_0 &= \alpha(1+\eta)\int_{\delta - S_{\mathrm{om}}}^{l} \tau(x)\,dx \\ &= \frac{\tau^{\mathrm{cr}}\alpha}{\omega}(1+\eta)\sinh(\omega x)\Big|_{\delta - S_{\mathrm{om}}}^{l} + \alpha(1+\eta)k_c(\delta - S_{\mathrm{om}})[l - (\delta - S_{\mathrm{om}})] \end{aligned} \tag{22}$$

or

$$\begin{aligned} \sigma_0 = \frac{\tau^{\mathrm{cr}}\alpha}{\omega}(1+\eta)\{\sinh(\omega l) - \sinh[\omega(\delta - S_{\mathrm{om}})]\} \\ + \alpha(1+\eta)k_c(\delta - S_{\mathrm{om}})[l - (\delta - S_{\mathrm{om}})]. \end{aligned} \tag{23}$$

2.3. Case 3 – Linear slip-softening model. Similar to Case 2, we find

$$\tau = \tau^{\mathrm{cr}} - k_c S, \quad \tau = \tau^{\mathrm{cr}} - k_c(u_f - u_m). \tag{24}$$

Slip stage.

$$S = \frac{\tau^{\mathrm{cr}}}{k_c}[1 - \cos(\omega x)]; \tag{25}$$

$$\sigma = \frac{\tau^{\mathrm{cr}}\alpha}{\omega}(1+\eta)\sqrt{2\frac{k_c S}{\tau^{\mathrm{cr}}} - \left(\frac{k_c S}{\tau^{\mathrm{cr}}}\right)^2}. \tag{26}$$

Pull-out stage.

$$S_{\mathrm{om}} = \frac{\tau^{\mathrm{cr}}}{k_c}[1 - \cos(\omega l)], \quad S = \frac{\tau^{\mathrm{cr}}}{k_c}[1 - \cos(\omega x)] + \delta - S_{\mathrm{om}}; \tag{27}$$

$$\sigma_{\mathrm{om}} = \frac{\tau^{\mathrm{cr}}\alpha}{\omega}(1+\eta)\sqrt{2\frac{k_c S_{\mathrm{om}}}{\tau^{\mathrm{cr}}} - \left(\frac{k_c S_{om}}{\tau^{\mathrm{cr}}}\right)^2}; \tag{28}$$

$$\tau = \tau^{\mathrm{cr}} - \tau^{\mathrm{cr}}[1 - \cos(\omega x)] - k_c(\delta - S_{\mathrm{om}}) = \tau^{\mathrm{cr}}\cos(\omega x) - k_c(\delta - S_{\mathrm{om}}); \tag{29}$$

$$\begin{aligned}\sigma_0 &= \alpha(1+\eta)\int_{\delta - S_{\mathrm{om}}}^{l} \tau(x)\,dx \\ &= \frac{\tau^{\mathrm{cr}}\alpha}{\omega}(1+\eta)\sin(\omega x)\Big|_{\delta - S_{\mathrm{om}}}^{l} - \alpha(1+\eta)k_c(\delta - S_{\mathrm{om}})[l - (\delta - S_{\mathrm{om}})]\end{aligned} \tag{30}$$

or

$$\begin{aligned}\sigma_0 = \frac{\tau^{\mathrm{cr}}\alpha}{\omega}(1+\eta)\{\sin(\omega l) - \sin[\omega(\delta - S_{\mathrm{om}})]\} \\ - \alpha(1+\eta)k_c(\delta - S_{\mathrm{om}})[l - (\delta - S_{\mathrm{om}})].\end{aligned} \tag{31}$$

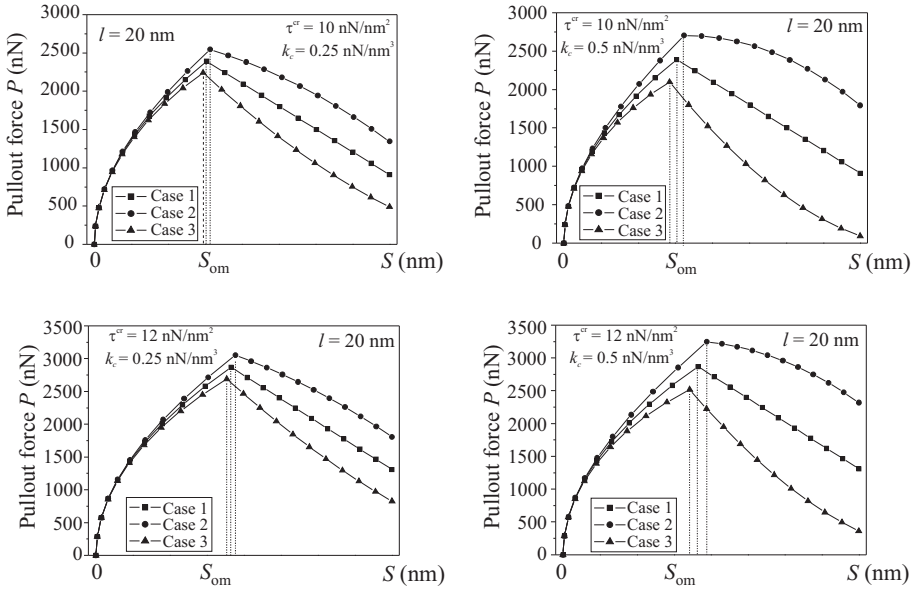

Fig. 3. Pullout force versus relative slip

3. Numerical example. The following geometrical and materials characteristics are used in the calculation (Fig. 3): $l = 20$ nm, $r_f = 1$ nm, $r_m = 10$ nm, $E_f = 1$ TPa, $E_m = 11.2$ GPa, $k_c = [0.25, 0.5]$ nN/nm^3, $\tau^{\rm cr} = [6, 12]$ nN/nm^2, $S_{\rm om} < \delta < l$, $P = A_f\sigma$, $P_{\rm pullout} = A_f\sigma_0$.

4. Conclusions. Based on the analysis performed, we may conclude that:

1. The increase of the value of $\tau^{\rm cr}$ within the range $[^{8,12}]$ yields increase of the value of $S_{\rm om}$ in all cases.

2. Keeping a constant value of $\tau^{\rm cr}$ and increasing the value of k_c into the range $[0.25, 0.5]$ results in that $S_{\rm om}$ remains constant in Case 1, increases in Case 2 and decreases in Case 3.

3. The maximal values of the pullout force remains constant in Case 1, increases in Case 2 and decreases in Case 3 with the increase of k_c.

REFERENCES

[1] Chena S. J., F. G. Collinsa, A. J. N. Macleoda, Z. Pana, W. H. Duana, C. M. Wanga. IES J. Part A: Civil & Structural Eng., **4**, 2011, No 4, 254–265.
[2] Makar J. M., J. J. Beaudoin. In: 1st Int. Symp. Nanotechnology in Construction, Paisley, Scotland, June 22–25, 2003, 331–341.
[3] Sanchez F. A., K. Sobolev. Construction and Building Materials, **24**, 2010, 2060–2071.
[4] Konsta-Gdoutos M. S., Z. S. Metaxa, S. P. Shah. Cement and Concrete Composites, **32**, 2010, No 2, 110–115.
[5] Tan Xiao, Kin Liao. Composites Part B: Engineering, **35**, 2004, No 3, 211–217.
[6] Xinyu Chen, I. J. Beyerlein, L. C. Brinson. J. Mech. Phys. Solids, **59**, 2011, 1938–1952.
[7] Xinyu Chen, I. J. Beyerlein, L. C. Brinson. Mechanics of Materials, **41**, 2009, 279–292.
[8] Xinyu Chen, I. J. Beyerlein, L. C. Brinson. Mechanics of Materials, **41**, 2009, 293–307.
[9] Chowdhury S. C., T. Okabe. Composites: Part A, **38**, 2007, 747–754.
[10] Xiaodong Hea, Chao Wanga, Liyong Tongb, Yibin Lia, Qingyu Penga, Lei Meia, Rongguo Wanga. Mechanics of Materials, **52**, 2012, 28–39.
[11] Zhang J., V. C. Li. Composites Science and Technology, **62**, 2002, No 6, 775–781.
[12] Li V. C., Y. Wang, S. Backer. Composites, **21**, 1990, No 2, 132–140.
[13] Lawrence P. J. Material Science, **7**, 1972, No 1, 1–6.
[14] Kazakov K., A. Yanakieva. Compt. rend. Acad. bulg. Sci., **65**, 2012, No 2, 219–224.
[15] Wang W., P. Ciselli, E. Kuznetsov, T. Peijs, A. H. Barber. Philos. Transact., Ser. A, Math. Phys. Eng. Sci., doi:10.1098/rsta.2007.2175 (published online).

[16] Nuriel S., A. Katz, H. D. Wagnera. Composites: Part A, **36**, 2005, 33–37.
[17] Barber A. H., S. R. Cohen, H. D. Wagnera. Appl. Phys. Lett., **82**, 2003, No 23, 4140–4142.
[18] Min-Feng Y., O. Lourie, M. J. Dyer, K. Moloni, T. F. Kelly, R. S. Ruoff. Science, **287**, 2000, 637–640.

Department of Mechanics of Materials
Instytut Podstawowych
Problemów Techniki (IPPT)
Polish Academy of Sciences
ul. Pawinskiego 5B
02-106 Warszawa, Poland

**Institute of Mechanics*
Bulgarian Academy of Sciences
Acad. G. Bonchev Str., Bl. 4
1113 Sofia, Bulgaria
e-mail: aniyanakieva@imbm.bas.bg